

ORIGINAL RESEARCH

Renal Denervation by Noninvasive Stereotactic Radiotherapy Induces Persistent Reduction of Sympathetic Activity in a Hypertensive Swine Model

Xingxing Cai, MD, PhD*; Yichen Shen, MM*; Yuli Yang, MD*; Wei Wang, MM; Li Qian, MM; Jing Cai, MB; Runmin Chi, MD; Shunxuan Yu, MB; Keke Li, MM; Zhixing Wei, MD, PhD; Taizhong Chen , MD, PhD; Yudong Fei, MD, PhD; Yaqin Han, MB; Xiu Chen, MB; Ming Liu, MM; Yifei Liu, MD; Dengbin Wang, MD, PhD; Mawei Jiang, MD, PhD; Yi-Gang Li , MD

BACKGROUND: We have previously reported the feasibility of noninvasive stereotactic body radiotherapy (SBRT) as a novel approach for renal denervation.

METHODS AND RESULTS: Herein, from a translational point of view, we assessed the antihypertensive effect and chronological evolution of SBRT-induced renal nerve injury within 6 months in a hypertensive swine model. Hypertension was induced in swine by subcutaneous implantation of deoxycorticosterone acetate pellets in combination with a high-salt diet. A single dose of 25 Gy with SBRT was delivered for renal denervation in 9 swine within 3.4±1.0 minutes. Blood pressure levels at baseline and 1 and 6 months post-SBRT were comparable to control (n=5), whereas renal norepinephrine was significantly lower at 6 months ($P<0.05$). Abdominal computed tomography, performed before euthanasia and renal function assessment, remained normal. Standard semiquantitative histological assessment showed that compared with control (1.4±0.4), renal nerve injury was greater at 1 month post-SBRT (2.3±0.3) and peaked at 6 months post-SBRT (3.2±0.8) ($P<0.05$), along with a higher proportion of active caspase-3–positive nerves ($P<0.05$). Moreover, SBRT resulted in continuous dysfunction of renal sympathetic nerves and low level of nerve regeneration in 6 months by immunohistochemistry analysis.

CONCLUSIONS: SBRT delivering 25 Gy for renal denervation was safe and related to sustained reduction of sympathetic activity by aggravating nerve damage and inhibiting nerve regeneration up to 6 months; however, its translation to clinical trial should be cautious because of the negative blood pressure response in the deoxycorticosterone acetate–salt hypertensive swine model.

Key Words: hypertension ■ nerve regeneration ■ noninvasive ■ renal denervation ■ stereotactic radioablation

Renal afferent and efferent nerves play a crucial role in cardiovascular, metabolic, and renal diseases, such as hypertension, atrial fibrillation, ventricular tachycardia, heart failure, obstructive sleep apnea, and renal failure.^{1–6} Catheter-based renal denervation (RDN) using endovascular radiofrequency or ultrasound is

the most extensively investigated invasive approach to reduce renal nerve signaling and thereby reduce systemic sympathetic activity. Noninvasive stereotactic body radiotherapy (SBRT), which delivers high-dose radiation precisely to target areas around bilateral renal arteries with a rapid dose falloff to minimize toxicity to

Correspondence to: Yi-Gang Li, MD, 1665 Kongjiang Rd, Shanghai 200092, China. E-mail: liyigang@xinhuamed.com.cn and Dengbin Wang, MD, PhD, 1665 Kongjiang Rd, Shanghai 200092, China. E-mail: wangdengbin@xinhuamed.com.cn

*Drs Cai, Shen and Yang are co–first authors.

Supplementary Material for this article is available at <https://www.ahajournals.org/doi/suppl/10.1161/JAHA.120.020068>.

For Sources of Funding and Disclosures, see page 11.

© 2021 The Authors. Published on behalf of the American Heart Association, Inc., by Wiley. This is an open access article under the terms of the Creative Commons Attribution-NonCommercial-NoDerivs License, which permits use and distribution in any medium, provided the original work is properly cited, the use is non-commercial and no modifications or adaptations are made.

JAHA is available at: www.ahajournals.org/journal/jaha

CLINICAL PERSPECTIVE

What Is New?

- Noninvasive stereotactic body radiotherapy, delivering a single dose of 25 Gy for renal denervation, induces sustainable reduction of sympathetic activity by aggravating nerve damage and inhibiting nerve regeneration within 6 months.
- Targeted treatment of branches or distal segment of the main renal artery adjacent to renal hilum advocated by radiofrequency renal denervation seems not appropriate for stereotactic body radiotherapy because of safety concerns.

What Are the Clinical Implications?

- Stereotactic body radiotherapy for renal denervation extends the horizon to treat hypertension.
- However, the optimal radiation dosage and plan to achieve sufficient efficacy and long-term safety require further investigation.

Nonstandard Abbreviations and Acronyms

DOCA	deoxycorticosterone acetate
GAP43	growth-associated protein 43
RDN	renal denervation
SBRT	stereotactic body radiotherapy

adjacent tissues, potentiated efficient renal nerve ablation by adopting appropriate radiation dosage.^{7,8}

Catheter-based RDN has achieved promising results of short-term efficacy to treat uncontrolled hypertension with or without concomitant antihypertensive medication.^{9–12} However, long-term durability data on contemporary devices and techniques used in second-generation sham-controlled trials are lacking. It was shown in preclinical studies that nerve injury after radiofrequency ablation peaked at 7 days, and maximum functional denervation sustained <30 days.¹³ It was also demonstrated that regenerative response could occur as early as 7 days after RDN.¹⁴ This phenomenon of nerve regeneration may lead to failure to maintain persistent decrease in sympathetic activity.¹⁵

Unlike catheter-based thermal injury, which induces immediate effects, SBRT-induced injury to relatively radioresistant nerves might take days to months to manifest fully.^{8,16} However, the mechanism and chronological evolution of SBRT-induced renal nerve injury remain to be elucidated. For further translational purpose, this study was therefore aimed to investigate the chronological evolution of treatment effects associated with stereotactic renal nerve radioablation using

standard histology and immunohistochemistry methods, and to explore the mechanism of high-dose radiation injury to renal nerves. Furthermore, we aimed to observe if this novel noninvasive RDN technique could lower blood pressure (BP) in a deoxycorticosterone acetate (DOCA)–salt hypertensive swine model and provide safety up to 6 months post-SBRT.

METHODS

The data that support the findings of this study are available from the corresponding author on reasonable request.

The experimental protocol was approved by Institutional Ethics Committee of Xinhua Hospital Affiliated to Shanghai Jiaotong University School of Medicine, and all animal procedures were performed in compliance with the *Guide for the Care and Use of Laboratory Animals*.

Study Design

A total of 14 Bama miniature swine, of both sexes, weighing from 20 to 25 kg, were randomly divided into a control group (n=5) and 2 treatment groups based on follow-up period post-SBRT: 1-month group (n = 4) and 6-month group (n = 5).

Hypertension was induced in control and 6-month groups by subcutaneous implantation of DOCA sustained-release pellets (100 mg/kg; Innovative Research of America) in combination with a high-salt diet.^{17,18} In 6-month group, RDN procedure was performed at 3 days after DOCA implantation. BP, blood urea nitrogen, and serum creatinine were measured at baseline and 1 and 6 months post-RDN in hypertensive animals.

At corresponding terminal time point, renal computed tomography (CT) angiography was performed before euthanasia. The kidneys were analyzed for norepinephrine levels by high-performance liquid chromatography–mass spectrometry. The renal arteries with associated nerves were evaluated by standard histopathology, immunohistochemistry, and apoptosis assay.

Anesthesia

All animals were fasted overnight with free access to water. After sedation with intramuscular Telazol (tiletamine and zolazepam) (4 mg/kg), anesthesia was then maintained through marginal ear vein with one half induction dosage every hour.

BP Measurement

BP was measured postanesthesia under the same conditions by a noninvasive tail-cuff system (BP-2010E;

Softron Biotechnology Ltd, Beijing, China). Three BP measurements were taken at 1-minute intervals, and average values were used for analysis.

SBRT Procedure for RDN

Animals received a single dose of 25 Gy delivered with SBRT to target areas around bilateral renal arteries. The general methods for SBRT contouring, planning, and delivery are provided in Data S1.

Terminal CT Evaluation

At predetermined terminal time point, abdominal contrast-enhanced CT scan was performed to assess possible radiation injuries to renal arteries and adjacent tissues. The evaluation was performed by 2 experienced radiologists blinded to the procedure on postprocessing Extended Brilliance Workspace (Philips Medical Systems, Cleveland, OH). Kidney dimensions and diameters of renal arteries at proximal, middle, and distal segments from hypertensive control and 6-month groups were measured using previous method.⁷

Necropsy

Animals were heparinized and humanely euthanized by intravenous injection of 10% potassium chloride after terminal CT scan. Gross examination of renal vessels and surrounding tissues was performed. Samples from proximal, middle, and distal regions of each kidney were rapidly harvested and frozen in liquid nitrogen for subsequent analysis of norepinephrine content using the method of high-performance liquid chromatography–mass spectrometry. Norepinephrine concentrations of left and right kidneys were averaged, and the percentage reduction compared with control was determined. Renal arteries were perfusion fixed and then the tissue block that included major vessels, renal lymph nodes, bilateral kidneys, ureters, and associated tissues was dissected and immersed in 4% paraformaldehyde.

Standard Histopathology

Renal arteries with surrounding tissues were cut at 3- to 4-mm intervals with 3 to 8 segments along the route of the artery, and enveloped in separate cassettes for dehydration and paraffin embedding. Sections (4 μ m thick) were cut on a rotary microtome and stained with hematoxylin and eosin, and those containing renal vessels were stained with additional Movat pentachrome stains. Periarterial organs adjacent to the renal hilum were also partially sectioned for assessment. Injury to renal nerves, vessels, arterioles, and surrounding soft tissues was evaluated using a standard semiquantitative scoring system of 0 to 4: 0 indicates none; 1, minimal; 2, mild; 3, moderate; and 4, severe.^{13,19}

To investigate the lesion depth and circumferential injury achieved with radioablation, the following parameters were analyzed: (1) maximum score of nerve change in separate regions of <2, 2 to 4, and >4 mm from arterial lumen; (2) maximum distance between arterial lumen and ablation zone; (3) number of quadrants with injured nerve fascicles (score ≥ 2)/number of quadrants with nerve fascicles; and (4) number of quadrants with injured periarterial soft tissue.

After grading all histological sections, the maximum injury score in each vessel was determined. Mean value of scores from bilateral vessels per animal was used for statistical analysis. Full details are shown in Data S1.

Apoptosis Assay

Random 4 sections from 4 different renal arteries in each group were detected for nerve apoptosis by immunostaining against active caspase-3 (dilution 1:400; 9661; Cell Signaling Technology, MA) and epifluorescence with a fluorescein isothiocyanate filter. Samples were costained with anti-S-100 antibody (dilution 1:100; ab868; Abcam, MA) conjugated to cy3-labeled goat anti-rabbit secondary antibody (dilution 1:500; A0516; Beyotime, Shanghai, China), and colocalization with active caspase-3 was used to quantify apoptotic nerves. The percentage of apoptotic nerves per section was calculated by number of active caspase-3-positive nerves divided by total number of nerves.

Immunohistochemistry

Consecutive sections from random 5 renal arteries in each group were selected for immunohistochemical stains against S-100 protein, a marker for recognition of nerve fascicles and tyrosine hydroxylase (dilution 1:100; ab112; Abcam, MA) and a functional indicator for norepinephrine synthesis. Presence of nerve sprouting after injury was assessed after immunostaining against GAP43 (growth-associated protein 43) (dilution 1:100; ab232772; Abcam). The intensity and distribution of staining against tyrosine hydroxylase and GAP43 were semiquantified using a scale of 0 to 3: 0 indicates no reaction; 1, patchy/very weak reaction; 2, weak to moderate reaction; and 3, strong reaction.^{13,19} Minimum score of each vessel was adopted for statistical analysis.

Statistical Analysis

Data are presented as mean \pm SD. Normality of distribution was tested with Shapiro-Wilk test. Comparisons of continuous variables with normal distribution were accomplished by unpaired Student *t* test for 2 groups, whereas variables with skewed distribution and ordinal data were compared with Mann-Whitney *U* test for 2 groups and Kruskal-Wallis test for >2 groups, followed, where appropriate, by all pairwise multiple comparisons.

Nerve injury scores in separate regions of <2, 2 to 4, and >4 mm from arterial lumen were analyzed by using 2-way ANOVA that included terms for group, distance, and group×distance interactions. ANOVA results were further analyzed by post hoc analysis using Bonferroni multiple comparison test. Spearman correlation was used to assess the correlation between radiation dosages and nerve injury scores. Two-sided $P<0.05$ was considered statistically significant. All analyses were performed with SPSS version 24 (IBM Corp, NY) and Prism 7 (GraphPad Software, CA).

RESULTS

Procedural Outcomes

SBRT was successfully performed for RDN in the treatment groups, and all 14 animals survived the expected-in-life phase of the study. Treatment characteristics are provided in Table S1. Figure 1 presents a typical RDN plan, showing that designated dose of 25 Gy precisely targeted areas around bilateral renal arteries with a rapid dose falloff to adjacent tissues. Total ablation target volume was 6.2 ± 1.0 mL. On-table treatment time was 3.4 ± 1.0 minutes.

BP and Renal Norepinephrine Concentration

Both systolic and diastolic BP significantly increased in control and 6-month groups since the first month after DOCA implantation, confirming successful establishment of hypertensive model. However, there were no

significant differences in BP at baseline and 1- and 6-month follow-up between the 2 groups (all $P>0.05$; Figure 2). Despite negative BP-lowering effect, SBRT resulted in a significant reduction of renal norepinephrine concentration at 6 months compared with control group (384.2 ± 103.6 versus 700.9 ± 121.8 ng/g; $P=0.002$).

Chronological Comparisons of Radiation-Induced Renal Nerve Injury

A total of 137 sections from 28 renal arteries were obtained, of which 13 sections were excluded because of incompleteness. Therefore, a total of 124 sections were used to analyze radiation-induced injury at different time points after SBRT. Nerve injury scores in treatment groups were significantly higher compared with control group (1.4 ± 0.4 ; $P<0.05$). Meanwhile, damage to renal nerves aggravated over time, and the score was significantly greater at 6 months compared with 1 month (3.2 ± 0.8 versus 2.3 ± 0.3 ; $P<0.05$; Figure 3A). At 1 month, the affected nerves were mainly characterized by degenerative changes, including vacuolization, digestion chambers, and nuclear pyknosis, as well as mild to moderate perineural inflammation, fibrosis, and collagen deposition. At 6 months, more nerve lesions were dominated by effacement of structure and calcification of necrotic endoneurium (Figure 3B). In addition, the proportion of apoptotic nerves increased gradually during the follow-up period, and was significantly higher at 6 months compared with control ($P<0.05$; Figure 4). Tyrosine hydroxylase staining scores for function of sympathetic nerves were significantly lower in treatment groups than in the untreated controls ($P<0.05$),

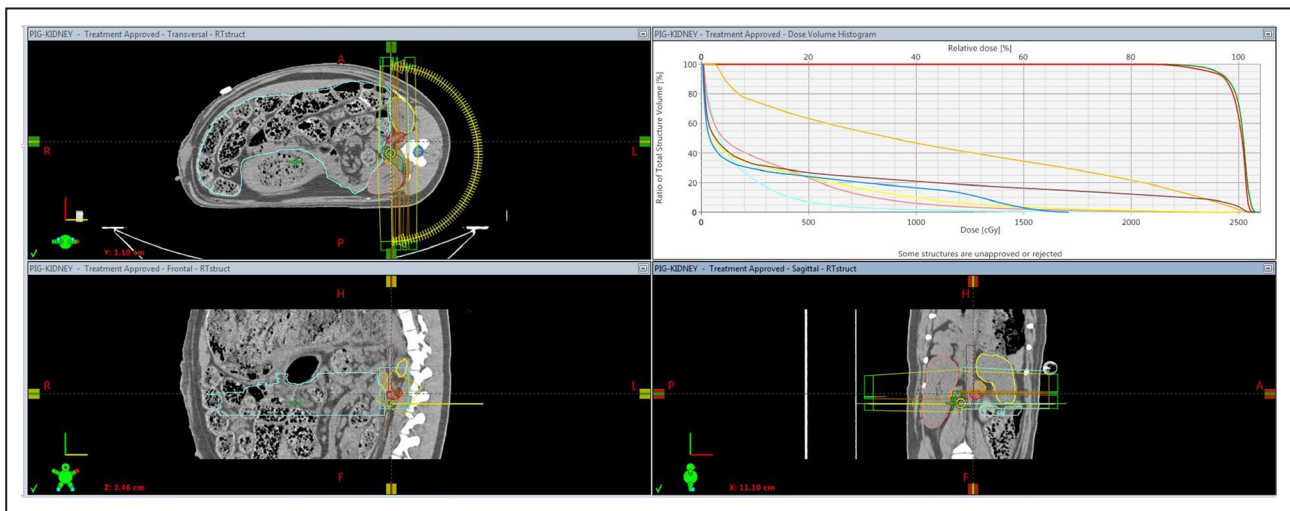


Figure 1. Screenshot of external beam planning system.

Axial (left top panel), sagittal (left lower panel), and coronal (right lower panel) views of contouring outcome and radiation delivery route (yellow arc in left top panel) of 25 Gy to radioablate renal nerves. Dose volume histogram (right top panel) demonstrates the designated dose concentrates on the planning target areas around the left (red) and right (green) renal arteries with a rapid dose falloff to adjacent critical structures, including left (yellow) and right (pink) kidneys, renal vein (orange), aorta (brown), spinal cord (dark blue), and bowel (light blue).

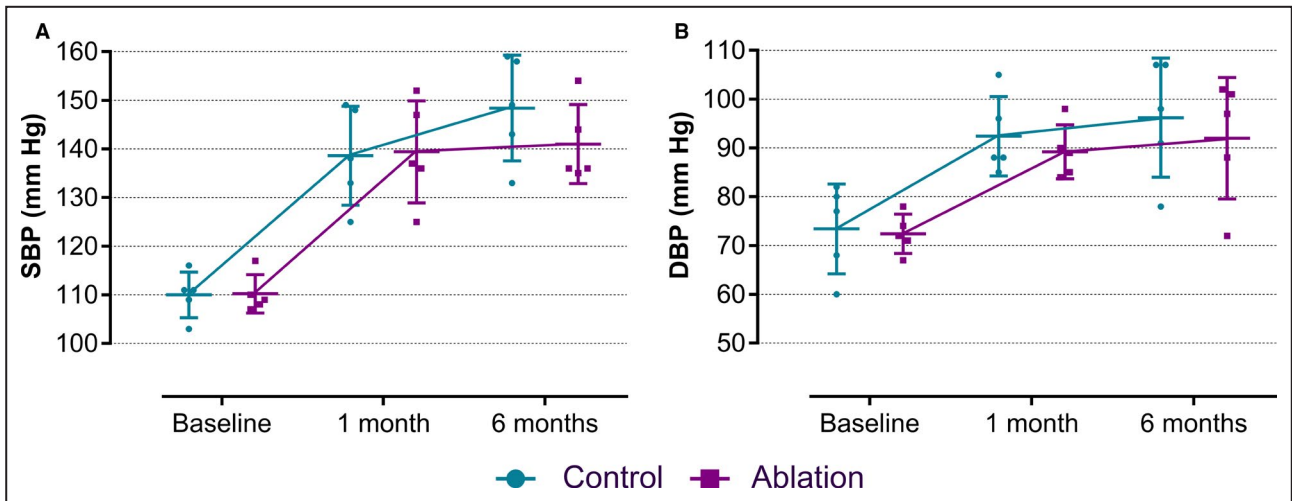


Figure 2. Blood pressure.

Systolic blood pressure (SBP) (A) and diastolic blood pressure (DBP) (B) at baseline and 1- and 6-month follow-up in control and 6-month ablation groups (mean±SD; n=5; unpaired Student *t* test).

whereas there was no significant difference in the staining intensity between different follow-up time points. Moreover, GAP43 for nerve regeneration showed similar weak expression at 1 and 6 months after SBRT compared with control group ($P>0.05$; Figure 5).

Characteristics of Radioablation in Circumference and Depth

Both treatment groups showed approximate 4 quadrants of injured tissue that demonstrates circumferential denervation, which is also reflected by similar results of injured nerve quadrants (score ≥ 2)/total quadrants with nerve fascicles close to 1. Meanwhile, the maximum distances from the arterial wall to the ablation zone were >10 mm, and there was no statistical difference between the 2 groups (all $P>0.05$; Table S2).

Despite sufficient penetration depth with SBRT, damage to renal nerves varied in separate regions of <2 , 2 to 4, and >4 mm from arterial lumen. At 1 month after treatment, nerve injury score in <2 -mm area was significantly higher compared with control group ($P<0.05$), whereas scores in 2- to 4- and >4 -mm areas were similar ($P>0.05$). At 6 months, scores in <2 - and 2- to 4-mm areas were greater in comparison to control ($P<0.05$), whereas mean scores in >4 -mm area were similar and <2 throughout 6-month follow-up (Figure 6A). Nerve injury scores at 6 months postprocedure in <2 -, 2- to 4-, and >4 -mm areas were significantly correlated with the minimum radiation dosages at isodose lines of approximate 2 mm (22.6 ± 1.6 Gy), 3 mm (20.2 ± 1.5 Gy), and 4 mm (12.6 ± 1.8 Gy) from arterial wall ($r=0.692$; $P=0.004$; Figure 6B and 6C).

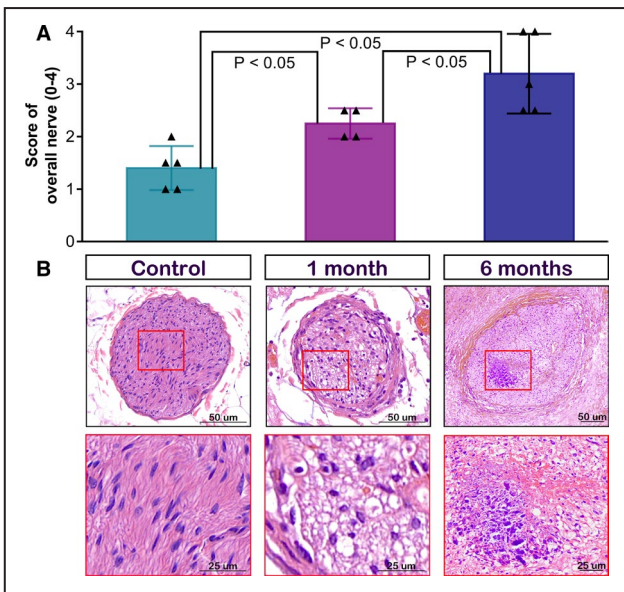


Figure 3. Chronological evolution of renal nerve injury.

A, Semiquantitative scores of nerve injury in control and treatment groups (mean±SD; n=4 for 1-month group and n=5 for the other groups; Kruskal-Wallis test, followed by all pairwise multiple comparisons). **B**, Representative images of nerves stained with hematoxylin and eosin at various time points (top) and magnified photomicrographs (bottom, red squares in top). Control nerves were chosen from untreated vessels at 6 months. Nerve fascicle at 1 month shows mild to moderate perineural fibrosis, vacuolization, and digestion chambers. Nerve fascicle at 6 months illustrates mild perineural fibrosis and calcification of necrotic endoneurium.

Safety Evaluation

Noninvasive safety evaluation consisted of blood test of renal function and CT angiography. All the swine successfully completed CT examination before euthanasia. Renal function, assessed by blood urea nitrogen and serum creatinine, remained consistent with control group during 6-month follow-up (all $P>0.05$; Figure S1). No apparent collateral damages to renal arteries,

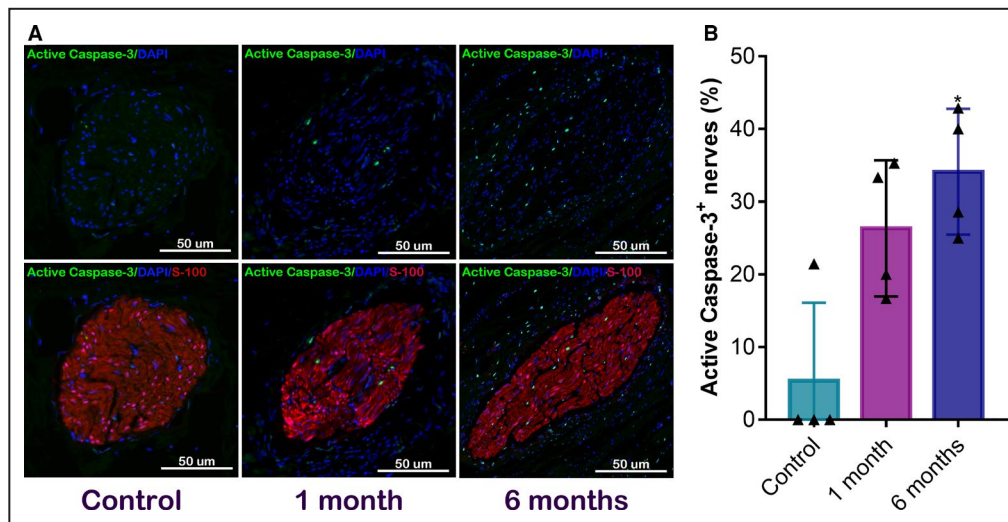


Figure 4. Renal nerve apoptosis.

A, Example images of active caspase-3–positive nerves in control and treatment groups. **B**, Quantitative analysis of renal nerve apoptosis (mean±SD; n=4; Kruskal-Wallis test, followed by all pairwise multiple comparisons). DAPI indicates 4',6-diamidino-2-phenylindole. * $P<0.05$ vs control.

kidneys, bowels, and other surrounding tissues were found on CT images within 6 months (Figure S2), and there were no significant differences in renal artery diameters and kidney dimensions between control and 6-month groups (all $P>0.05$; Table S3).

On gross specimen examination, the extent of connective tissue adherence along the route of treated renal arteries increased in a time-dependent manner. No discernible adverse effects were seen outside the treatment zone, including kidneys, ureters, adrenal glands, psoas muscle, bowel, liver, spleen, stomach, and pancreas.

Table 1 and Figure 7 show comparison of arterial and periarterial tissue injury between treatment groups. Endothelial loss was not observed in both groups. Minimal focal eccentric neointima was formed on the internal elastic lamina of 5 of 10 renal arteries at 6 months. Renal arterial medial depth and circumferential injury, reflected by proteoglycan replacement of smooth muscle cell loss, were occasionally seen at 6 months, whereas no medial thinning was found. Meanwhile, damage to renal vein was absent throughout 6 months. Arteriolar injury score was significantly greater at 6 months compared with 1 month ($P<0.05$). Arteriolar damage at 1 month was characterized by mild perivascular inflammation and smooth muscle cell loss, whereas at 6 months, it was characterized by more fibrinoid necrosis. In addition, arteriolar occlusion attributable to intimal hyperplasia and thrombosis was frequently observed at 6 months. Although there seems to be a trend showing more severe soft tissue injury characterized by denatured collagen, fat

necrosis, and fibrosis at 6 months in comparison to 1 month post-SBRT, no statistical difference was found between groups ($P>0.05$).

Damage to adjacent organs by radioablation with 25 Gy in 6 months was scarce by histopathological analysis. Focal ureteral epithelial vacuolization and mild chronic intestinal inflammation were occasionally observed after treatment. At 6 months post-SBRT, obvious radiation injury, characterized by focal glomerular vitreous degeneration, disappearance of renal tubules with inflammatory cell infiltration, interstitial fibrous tissue hyperplasia, and collagen degeneration, was evidenced in a small proportion of one kidney (Figure S3).

DISCUSSION

SBRT has been investigated as a novel technique for noninvasive RDN in preclinical studies,^{7,8} and radiation energy at 25 Gy appears to be an appropriate effective and safe dosage up to 3 months. However, damage to renal nerves with SBRT seems to be relatively mild in early stages compared with catheter-based RDN.⁷ In current study, we provide evidence, for the first time, that radiation-induced renal nerve injury aggravated over time, resulting from direct effects of irradiation and secondary effects of regional fibrosis and damaged microvasculature, which induced nerve apoptosis and necrosis, as well as inhibition of nerve regeneration simultaneously. Moreover, SBRT successfully reduced renal sympathetic activity with a favorable safety performance up to 6 months, despite

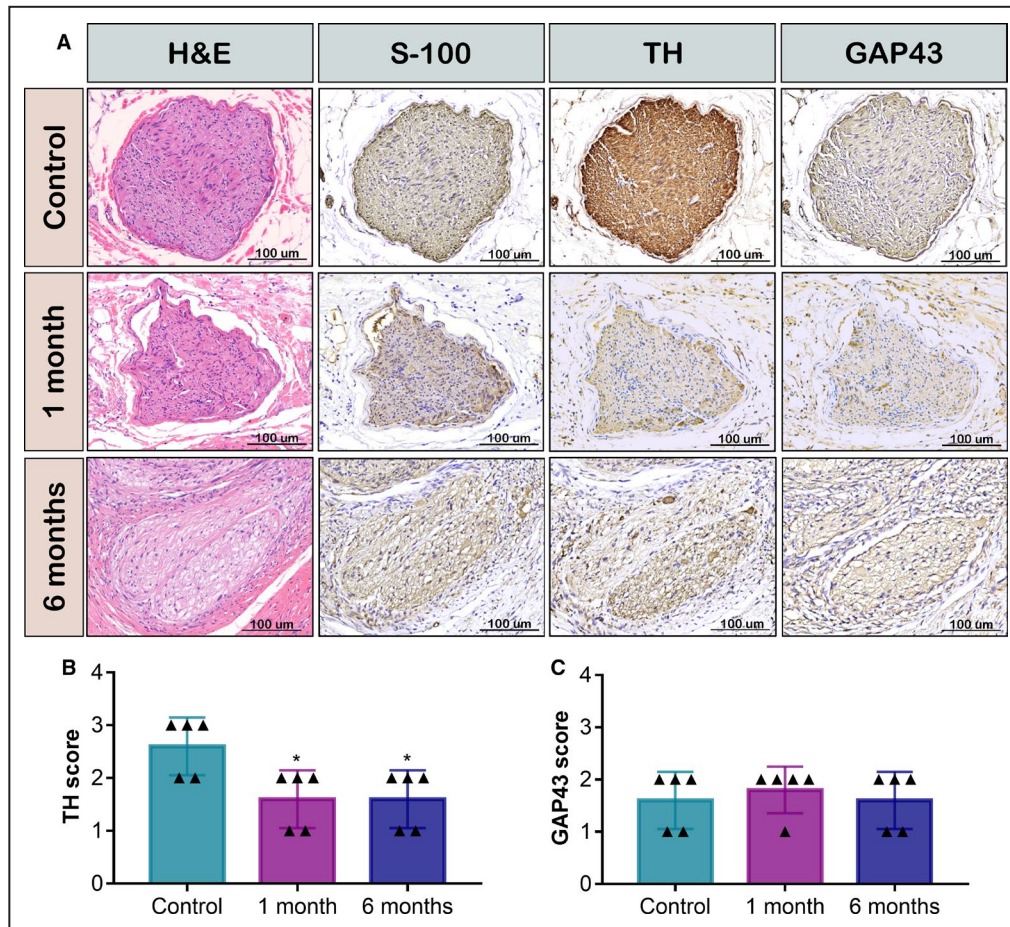


Figure 5. Immunohistochemistry of renal nerves.

A, Representative micrographs of untreated normal nerve and ablated nerves at 1 and 6 months postprocedure with hematoxylin and eosin (H&E) and immunohistochemical stains against S-100, tyrosine hydroxylase (TH), and GAP43 (growth-associated protein 43). Positive reaction to S-100 confirms the presence of nerve fascicles. Compared with strong TH staining in normal nerve, decreased expression of TH, which demonstrates functional nerve damage, is continuously observed in treated nerves, whereas GAP43 expression, an indicator for nerve regeneration, remains weak throughout 6 months. Semiquantitative scores of TH (**B**) and GAP43 (**C**) in control and treatment groups (mean±SD; n=5; Kruskal-Wallis test, followed by all pairwise multiple comparisons). **P*<0.05 vs control.

failure to lower BP in the DOCA-salt hypertensive swine model.

Chronological Evolution of SBRT-Induced Renal Nerve Injury

Anatomic regrowth of renal nerves in human has been demonstrated after kidney transplantation, developing in association with clinical hypertension.²⁰ In preclinical studies, regenerative response of injured renal nerve was observed as early as 7 days following radiofrequency RDN,¹⁴ and maximum functional denervation sustained <30 days,¹³ followed by complete reinnervation at 11 months.¹⁵ In contrast to catheter-based RDN, stereotactic renal nerve radioablation

exhibited entirely different chronological evolution of denervation. SBRT concentrates high-dose radiation to the target and mediates direct damage by inducing DNA double-strand breaks, resulting in cell death during division. Therefore, the mature nerve is relatively resistant to the direct cytotoxic effects of radiation and may show limited early damage, but late effects can be manifested to considerable and varying degrees.¹⁶ In this study, after delivery with a single dose of 25 Gy for RDN, the early pathological manifestations of renal nerves were mainly characterized by degenerative changes, including vacuolization and digestion chambers. In the later stages, more advanced changes of nerves with effacement of structure were observed, and the regenerative response

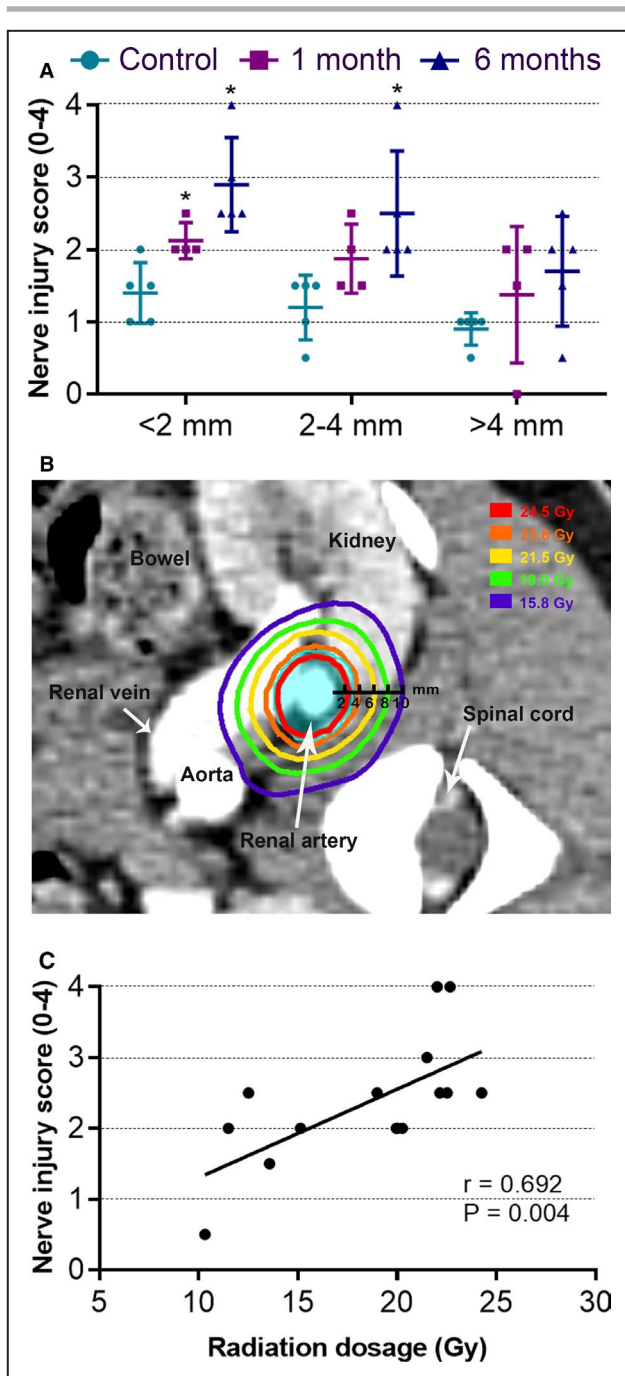


Figure 6. Radiation-induced denervative effect in depth. **A**, Semiquantitative scores of nerve injury in separate regions of <2, 2 to 4, and >4 mm from arterial lumen in control and treatment groups (mean±SD; n=4 for 1-month group and n=5 for the other groups; 2-way ANOVA, between group; Bonferroni multiple comparison test). *P<0.05 vs control. **B**, Treatment plan example of renal nerve radioablation with 25 Gy in axial plane of contrast-enhanced computed tomography scan, showing colored isodose lines at approximate distances of 2, 4, 6, 8, and 10 mm from renal arterial lumen. The planning target volume is highlighted in cyan; and red, orange, yellow, green, and blue curves indicate the distribution of zones receiving doses of at least 24.5, 23.6, 21.5, 19.0, and 15.8 Gy, respectively. **C**, Spearman correlation between nerve injury scores at 6 months postprocedure in <2-, 2- to 4-, and >4-mm areas and the minimum radiation dosages at isodose lines of 2, 3, and 4 mm from arterial wall.

of fibrous connective tissue rather than proliferation of Schwann cells.^{21,22} In accordance with previous results, this research found that arteriolar damage at 6 months after radioablation was characterized by more fibrinoid necrosis and occlusion attributable to intimal hyperplasia and thrombosis. Meanwhile, the extent of connective tissue adherence along the route of treated renal arteries increased in a time-dependent manner. Hence, it could conceivably be hypothesized that besides direct radiation damage to renal nerves, progressive interstitial fibrosis in the later stage oppresses the nerves, and ischemia secondary to arteriolar stenosis or occlusion induces nerve apoptosis and necrosis. Furthermore, hypoxia and fibrosis can inhibit Schwann cell and axon regeneration, promoting further demyelination, axonal degeneration, and nerve fiber loss.

Dependent Factors of Denervation Efficiency by SBRT

Soft tissue is radiosensitive so that its damage, characterized by fat necrosis and fibrosis, appeared in the early stage after radioablation. Although the average maximum lesion depth measured from the renal arterial wall to the border of injured soft tissue extended beyond 10 mm throughout 6 months, damage to renal nerves varied within different distances. In comparison to the gradual aggravation of neural degeneration and necrosis in <4-mm area, nerve injury outside 4 mm seemed relatively mild. This discrepancy could be attributed to the scheme of SBRT plan. In current study, planning target volume was derived from an isotropic 3-mm expansion on internal target volume. The designated dose of 25 Gy covered most region of planning target volume and declined rapidly away from the target. According to the results of prior animal studies about peripheral neuropathy following intraoperative radiotherapy, the effective dose for 50% of nerve fiber loss is 25.3 Gy,²² and doses of <20 Gy may not result in significant nerve injury.^{21,23} Therefore, current SBRT

remained at a low level, which could not effectively restore the ability to synthesize norepinephrine, suggesting that SBRT may have a long-term advantage in reducing sympathetic activity.

Mechanism of Sustained Renal Nerve Injury

Several reports in the field of intraoperative radiotherapy have shown that microvasculature may play a crucial part in the induction of delayed radiation injury. Damaged microvasculature would favor proliferation

Table 1. Semiquantitative Scores of Arterial and Periarterial Tissue Injury

Variable	1 mo	6 mo	P value
Renal artery			
Endothelial loss	0±0	0±0	...
Medial depth changes	0±0	1.4±1.9	0.173
Medial thinning (score 0–1)	0±0	0±0	...
Medial circumferential changes	0±0	0.8±1.2	0.173
Neointimal area, mm ²	0±0	0.19±0.23	0.083
Renal vein			
Endothelial loss	0±0	0±0	...
Medial depth changes	0±0	0±0	...
Medial circumferential changes	0±0	0±0	...
Arteriole injury	1.6±0.6	2.4±0.2	0.043
Soft tissue injury	2.0±1.4	3.1±0.2	0.068

Values are expressed as mean±SD, based on a scale of 0 to 4, unless otherwise stated. P value was calculated from Mann-Whitney U test.

regimen cannot denervate sufficiently in >4-mm area that received radiation of <20 Gy, and this may explain why the decrease of renal norepinephrine concentration by radioablation in this study was smaller than that achieved with transcatheter RDN methods.^{7,24,25} Another possible explanation for this is that SBRT with 25 Gy induces relatively mild early injury to renal nerves even in <4-mm zone, in contrast to immediate devastating effect by radiofrequency or ultrasound.^{13,26}

Impact on DOCA-Induced Hypertension

DOCA combined with high-salt diet is a common method to establish a hypertensive animal model that exhibits elevated sympathetic activity.^{17,27} However, some studies indicate that intact renal nerves are unnecessary for the onset or maintenance of DOCA-salt hypertension.^{27,28} In our study, RDN with SBRT failed to lower BP during 6-month follow-up. A possible explanation might be attributable to inadequate denervation and relatively mild reduction of renal norepinephrine concentration with current SBRT scheme. Furthermore, RDN alone may not completely prevent DOCA-induced BP increase. Besides sympathetic mechanism, other mechanisms, including sodium retention and the direct effect on vessels, are responsible for DOCA-induced hypertension.^{27,29}

Safety Concerns

In addition to efficacy for RDN, SBRT maintained a favorable safety performance within 6 months. As mentioned in previous literature, great vessel may tolerate up to 30 Gy without significant complication.¹⁶ Accordingly, at 6 months after radioablation with 25 Gy in this study, no vascular complications, such as renal artery stenosis, thrombosis, fibrotic occlusion, and aneurysm, were found on CT images, notwithstanding histological evidence of mild medial injury and focal

eccentric neointimal formation on the internal elastic lamina, which was also observed in preclinical studies of radiofrequency RDN.³⁰ However, rare renal artery stenosis was reported up to 3 years follow-up after radiofrequency RDN.^{31,32}

Although dose tolerance limits for abdominal organs with hypofractionation are still uncertain, radiation to closely related structures can be limited to safe levels with this novel technique for RDN based on early toxicity data in the field of intraoperative radiotherapy.¹⁶ The dose and total volume of critical normal structures that receive radiation can be used to predict the potential likelihood of long-term toxicity. In a clinical study delivering 26 Gy in one fraction to treat renal cell carcinoma with a median planning target volume of 77.2 mL, no treatment-related grade ≥3 intestinal toxicities were recorded during a median follow-up of 2 years.³³ Consistent with previous findings, no apparent collateral damage to organs surrounding the treated renal arteries was observed on CT images within 6 months after delivery of 25 Gy to the 6.2±1.0 mL target volume. In addition, renal function remained within the normal range, despite occasional pathological findings of kidney injury and focal ureteral epithelial vacuolization. Hence, it seems that targeted treatment of branches or distal segment of the main renal artery adjacent to renal hilum advocated by radiofrequency RDN is not appropriate for current methods.

Clinical Implications

Taken together, these findings suggest SBRT with appropriate dosage and radiation plan is feasible for RDN and could result in sustained reduction of sympathetic activity up to 6 months postprocedure. Compared with catheter-based RDN, SBRT has several advantages, as follows: First, there is no need for anesthesia and puncture of femoral artery, which

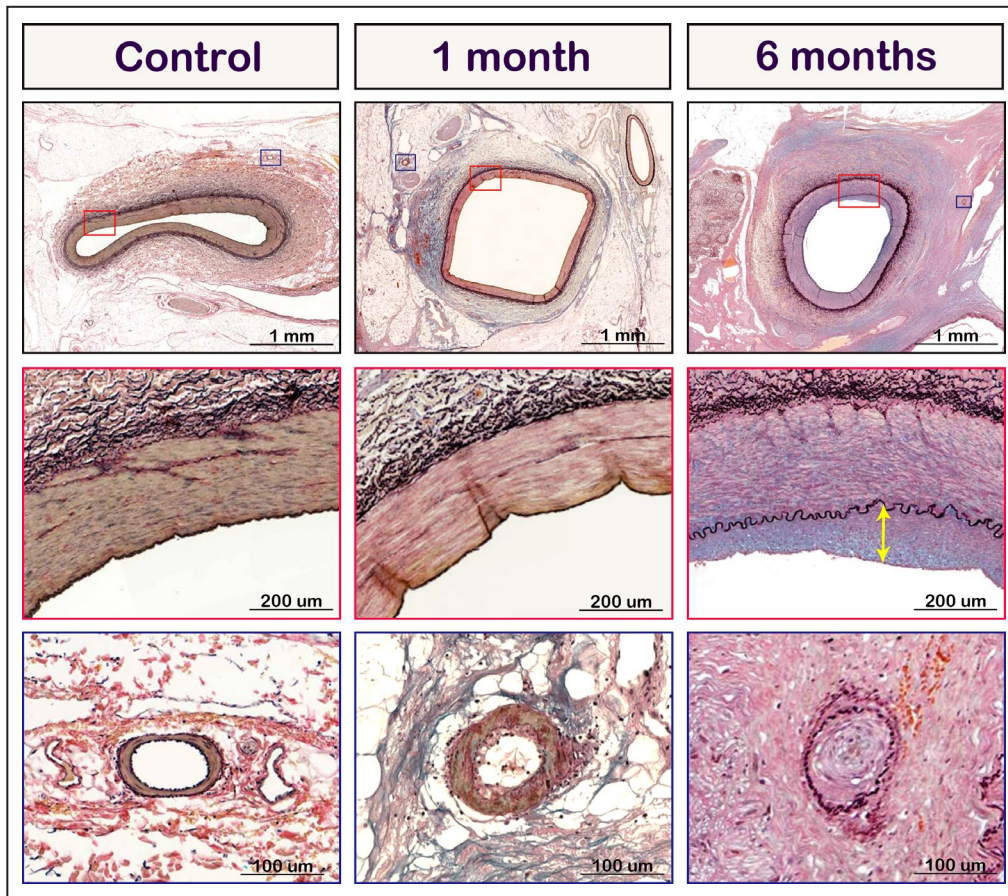


Figure 7. Renal arterial and periarterial tissue injury.

(**Top**) Representative images of renal arteries and circumferential area stained with Movat pentachrome in control and treatment groups. Magnified photomicrographs of renal arteries (**middle**, red squares in **top**) and arterioles (**bottom**, blue squares in **top**). Renal arteries at 1 month show no apparent medial injury, whereas mild proteoglycan replacement of smooth muscle cell loss, which stains green, is occasionally found at 6 months. Minimal eccentric thickening of neointima (injury) formed on the internal elastic lamina is observed at 6 months after ablation. Arterioles at 1 month show mild perivascular inflammation and smooth muscle cell loss. Arteriolar occlusion, induced by intimal hyperplasia and thrombosis, is frequently observed at 6 months.

avoids complications related to catheterization, such as femoral artery hematoma, pseudoaneurysm, and renal artery dissection. Second, externally delivered radiation has no anatomical restrictions in terms of renal artery length and diameter, accessory artery, and prior stent implantation, despite limitation to ablate the arterial branches near the renal hilum. Third, in contrast to dependency of operator's experience during endovascular procedure, radiologists and cardiologists can individualize SBRT plan based on CT images before treatment, minimizing radiation to adjacent organs while ensuring denervation by covering appropriate circumferential distance. Fourth, linear accelerators delivering high-dose rate and flattening filter-free beams by volumetric modulated arc therapy can reduce treatment time to a few minutes, so that it will improve patient comfort and reduce motion during treatment, providing an overall accuracy.³⁴ Fifth,

the characteristic of radiation damage to renal nerves aggravating over time with impaired regenerative capacity provides the advantage of sustained reduction of sympathetic activity. However, this noninvasive technique also has some shortcomings, including mild nerve injury in the early stage, unsuitability for selective denervation guided by renal nerve stimulation,³⁵ and absence of a periprocedural marker for successful ablation.

Study Limitations

The findings of this swine study should be interpreted with caution because the underlying arteriosclerosis in patients with hypertension may respond differently to radiation, and regenerative response of damaged renal nerves in human may be inconsistent. Furthermore, DOCA-salt hypertensive model cannot completely simulate multifactorial essential hypertension, and

noninvasive BP measurement may be influenced by anesthesia. Finally, despite a favorable safety profile within 6 months, delayed radiation injury may take months to years, so safety data with longer follow-up are required.

CONCLUSIONS

SBRT delivering a single dose of 25 Gy for RDN maintains a promising safety profile with sustainable reduction of sympathetic activity by aggravating nerve damage and inhibiting nerve regeneration within 6 months. Despite its limitations, including relatively mild denervation in the early stage and unsuitability for ablation of renal arterial branches adjacent to renal hilum, stereotactic renal nerve radioablation extends the horizon in therapeutics of diseases related to overactivated sympathetic tone. Further investigation is warranted about the optimal radiation dosage and plan to achieve sufficient efficacy and long-term safety.

ARTICLE INFORMATION

Received November 5, 2020; accepted June 22, 2021.

Affiliations

Department of Cardiology (X.C., Y.Y., Z.W., T.C., Y.F., Y.H., X.C., Y.L.), and Department of Oncology (Y.S., W.W., S.Y., K.L., M.J.), Xinhua Hospital Affiliated to Shanghai Jiaotong University School of Medicine, China; Department of Pathology, Affiliated Hospital of Nantong University, China (L.Q., Y.L.); and Department of Radiology, Xinhua Hospital Affiliated to Shanghai Jiaotong University School of Medicine, China, (J.C., R.C., M.L., D.W.).

Sources of Funding

This work was supported by the grants from the State Key Program of National Natural Science Foundation of China (No. 81530015); and the Scientific Research Project of Shanghai Science and Technology Committee (No. 19411963500).

Disclosures

None.

Supplementary Material

Data S1
Tables S1–S3
Figures S1–S3

REFERENCES

- DeLalio LJ, Sved AF, Stocker SD. Sympathetic nervous system contributions to hypertension: updates and therapeutic relevance. *Can J Cardiol*. 2020;36:712–720. DOI: 10.1016/j.cjca.2020.03.003.
- Steinberg JS, Shabanov V, Ponomarev D, Losik D, Ivanickiy E, Kropotkin E, Polyakov K, Ptaszynski P, Keweloh B, Yao CJ, et al. Effect of renal denervation and catheter ablation vs catheter ablation alone on atrial fibrillation recurrence among patients with paroxysmal atrial fibrillation and hypertension: the ERADICATE-AF randomized clinical trial. *JAMA*. 2020;323:248–255. DOI: 10.1001/jama.2019.21187.
- Bradfield JS, Hayase J, Liu K, Moriarty J, Kee ST, Do D, Ajijola OA, Vaseghi M, Gima J, Sorg J, et al. Renal denervation as adjunctive therapy to cardiac sympathetic denervation for ablation refractory ventricular tachycardia. *Heart Rhythm*. 2020;17:220–227. DOI: 10.1016/j.hrthm.2019.09.016.
- Fukuta H, Goto T, Wakami K, Kamiya T, Ohte N. Effects of catheter-based renal denervation on heart failure with reduced ejection fraction: a meta-analysis of randomized controlled trials [published online ahead of print May 11, 2020]. *Heart Fail Rev*. DOI: 10.1007/s10741-020-09974-4.
- Venkataraman S, Vungarala S, Covassin N, Somers VK. Sleep apnea, hypertension and the sympathetic nervous system in the adult population. *J Clin Med*. 2020;9:591. DOI: 10.3390/jcm9020591.
- Noh MR, Jang HS, Kim J, Padanilam BJ. Renal sympathetic nerve-derived signaling in acute and chronic kidney diseases. *Int J Mol Sci*. 2020;21:1647. DOI: 10.3390/ijms21051647.
- Cai X, Yang Y, Shen Y, Wang W, Qian LI, Cai J, Chi R, Fei Y, Yu S, Wei LE, et al. Noninvasive stereotactic radiotherapy for renal denervation in a swine model. *J Am Coll Cardiol*. 2019;74:1697–1709. DOI: 10.1016/j.jacc.2019.07.053.
- Bhatt N, Long SA, Gardner EA, Tay J, Ladich E, Chamberlain D, Fogarty TJ, Maguire PJ. Radiosurgical ablation of the renal nerve in a porcine model: a minimally invasive therapeutic approach to treat refractory hypertension. *Cureus*. 2017;9:e1055. DOI: 10.7759/cureus.1055.
- Townsend RR, Mahfoud F, Kandzari DE, Kario K, Pocock S, Weber MA, Ewen S, Tsioufis K, Tousoulis D, Sharp ASP, et al. Catheter-based renal denervation in patients with uncontrolled hypertension in the absence of antihypertensive medications (SPYRAL HTN-OFF MED): a randomised, sham-controlled, proof-of-concept trial. *Lancet*. 2017;390:2160–2170. DOI: 10.1016/S0140-6736(17)32281-X.
- Azizi M, Schmieder RE, Mahfoud F, Weber MA, Daemen J, Davies J, Basile J, Kirtane AJ, Wang Y, Lobo MD, et al. Endovascular ultrasound renal denervation to treat hypertension (RADIANCE-HTN SOLO): a multicentre, international, single-blind, randomised, sham-controlled trial. *Lancet*. 2018;391:2335–2345. DOI: 10.1016/S0140-6736(18)31082-1.
- Kandzari DE, Böhm M, Mahfoud F, Townsend RR, Weber MA, Pocock S, Tsioufis K, Tousoulis D, Choi JW, East C, et al. Effect of renal denervation on blood pressure in the presence of antihypertensive drugs: 6-month efficacy and safety results from the SPYRAL HTN-ON MED proof-of-concept randomised trial. *Lancet*. 2018;391:2346–2355. DOI: 10.1016/S0140-6736(18)30951-6.
- Böhm M, Kario K, Kandzari DE, Mahfoud F, Weber MA, Schmieder RE, Tsioufis K, Pocock S, Konstantinidis D, Choi JW, et al. Efficacy of catheter-based renal denervation in the absence of antihypertensive medications (SPYRAL HTN-OFF MED Pivotal): a multicentre, randomised, sham-controlled trial. *Lancet*. 2020;395:1444–1451. DOI: 10.1016/S0140-6736(20)30554-7.
- Sakakura K, Tunek S, Yahagi K, O'Brien AJ, Ladich E, Kolodgie FD, Melder RJ, Joner M, Virmani R. Comparison of histopathologic analysis following renal sympathetic denervation over multiple time points. *Circ Cardiovasc Interv*. 2015;8:e001813. DOI: 10.1161/CIRCINTERVENTIO NS.114.001813.
- Rousselle SD, Brants IK, Sakaoka A, Hubbard B, Jackson ND, Wicks JR, Dillon KN, Naiche LA, Hart R, Garza JA, et al. Neuromatous regeneration as a nerve response after catheter-based renal denervation therapy in a large animal model: immunohistochemical study. *Circ Cardiovasc Interv*. 2015;8:e002293. DOI: 10.1161/CIRCINTERVENTIO NS.114.002293.
- Booth LC, Nishi EE, Yao ST, Ramchandra R, Lambert GW, Schlaich MP, May CN. Reinnervation of renal afferent and efferent nerves at 5.5 and 11 months after catheter-based radiofrequency renal denervation in sheep. *Hypertension*. 2015;65:393–400. DOI: 10.1161/HYPERTENSIO NAHA.114.04176.
- Sindelar WF, Kinsella TJ. Normal tissue tolerance to intraoperative radiotherapy. *Surg Oncol Clin N Am*. 2003;12:925–942. DOI: 10.1016/S1055-3207(03)00087-5.
- Han W, Fang W, Gan Q, Guan S, Li Y, Wang M, Gong K, Qu X. Low-dose sustained-release deoxycorticosterone acetate-induced hypertension in Bama miniature pigs for renal sympathetic nerve denervation. *J Am Soc Hypertens*. 2017;11:314–320. DOI: 10.1016/j.jash.2017.02.006.
- Schwarzl M, Hamdani N, Seiler S, Alogna A, Manninger M, Reilly S, Zirngast B, Kirsch A, Steendijk P, Verderber J, et al. A porcine model of hypertensive cardiomyopathy: implications for heart failure with preserved ejection fraction. *Am J Physiol Heart Circ Physiol*. 2015;309:1407–1418. DOI: 10.1152/ajpheart.00542.2015.
- Sakakura K, Ladich E, Edelman ER, Markham P, Stanley JR, Keating J, Kolodgie FD, Virmani R, Joner M. Methodological standardization for the pre-clinical evaluation of renal sympathetic denervation. *JACC Cardiovasc Interv*. 2014;7:1184–1193. DOI: 10.1016/j.jcin.2014.04.024.

20. Mauriello A, Rovella V, Borri F, Anemona L, Giannini E, Giacobbi E, Saggini A, Palmieri G, Anselmo A, Bove P, et al. Hypertension in kidney transplantation is associated with an early renal nerve sprouting. *Nephrol Dial Transplant*. 2017;32:1053–1060. DOI: 10.1093/ndt/gfx069.
21. Vujaskovic Z, Gillette SM, Powers BE, LaRue SM, Gillette EL, Borak TB, Scott RJ, Colacchio TA. Intraoperative radiation (IORT) injury to sciatic nerve in a large animal model. *Radiother Oncol*. 1994;30:133–139. DOI: 10.1016/0167-8140(94)90042-6.
22. Vujaskovic Z, Powers BE, Paardekooper G, Gillette SM, Gillette EL, Colacchio TA. Effects of intraoperative irradiation (IORT) and intraoperative hyperthermia (IOHT) on canine sciatic nerve: histopathological and morphometric studies. *Int J Radiat Oncol Biol Phys*. 1999;43:1103–1109. DOI: 10.1016/S0360-3016(98)00529-X.
23. Kinsella TJ, DeLuca AM, Barnes M, Anderson W, Terrill R, Sindelar WF. Threshold dose for peripheral neuropathy following intraoperative radiotherapy (IORT) in a large animal model. *Int J Radiat Oncol Biol Phys*. 1991;20:697–701. DOI: 10.1016/0360-3016(91)90011-R.
24. Tzafiri AR, Mahfoud F, Keating JH, Spognardi AM, Markham PM, Wong G, Highsmith D, O'Fallon P, Fuimaono K, Edelman ER. Procedural and anatomical determinants of multielectrode renal denervation efficacy. *Hypertension*. 2019;74:546–554. DOI: 10.1161/HYPERTENSIONAHA.119.12918.
25. Pathak A, Coleman L, Roth A, Stanley J, Bailey L, Markham P, Ewen S, Morel C, Despas F, Honton B, et al. Renal sympathetic nerve denervation using intraluminal ultrasound within a cooling balloon preserves the arterial wall and reduces sympathetic nerve activity. *EuroIntervention*. 2015;11:477–484. DOI: 10.4244/EIJV1114A96.
26. Sakakura K, Roth A, Ladich E, Shen K, Coleman L, Joner M, Virmani R. Controlled circumferential renal sympathetic denervation with preservation of the renal arterial wall using intraluminal ultrasound: a next-generation approach for treating sympathetic overactivity. *EuroIntervention*. 2015;10:1230–1238. DOI: 10.4244/EIJY14M10_14.
27. Thomas GD, O'Hagan KP, Zambraski EJ. Chemical sympathectomy alters the development of hypertension in miniature swine. *Hypertension*. 1991;17:357–362. DOI: 10.1161/01.HYP.17.3.357.
28. Dzielak DJ, Norman RA. Renal nerves are not necessary for onset or maintenance of DOC-salt hypertension in rats. *Am J Physiol*. 1985;249:945–949.
29. Gomez-Sanchez EP. DOCA/salt: much more than a model of hypertension. *J Cardiovasc Pharmacol*. 2019;74:369–371. DOI: 10.1097/FJC.0000000000000753.
30. Sakaoka A, Rouselle SD, Hagiwara H, Tellez A, Hubbard B, Sakakura K. Safety of catheter-based radiofrequency renal denervation on branch renal arteries in a porcine model. *Catheter Cardiovasc Interv*. 2019;93:494–502. DOI: 10.1002/ccd.27953.
31. Mahfoud F, Böhm M, Schmieder R, Narkiewicz K, Ewen S, Ruilope L, Schlaich M, Williams B, Fahy M, Mancia G. Effects of renal denervation on kidney function and long-term outcomes: 3-year follow-up from the Global SYMPLICITY Registry. *Eur Heart J*. 2019;40:3474–3482. DOI: 10.1093/eurheartj/ehz118.
32. Townsend RR, Walton A, Hettrick DA, Hickey GL, Weil J, Sharp ASP, Blankenstijn PJ, Böhm M, Mancia G. Incidence of renal artery damage following percutaneous renal denervation with radio frequency renal artery ablation systems: review and meta-analysis of published reports. *EuroIntervention*. 2020;16:89–96. DOI: 10.4244/EIJ-D-19-00902.
33. Siva S, Pham D, Kron T, Bressel M, Lam J, Tan TH, Chesson B, Shaw M, Chander S, Gill S, et al. Stereotactic ablative body radiotherapy for inoperable primary kidney cancer: a prospective clinical trial. *BJU Int*. 2017;120:623–630. DOI: 10.1111/bju.13811.
34. Barbiero S, Rink A, Matteucci F, Fedele D, Paiar F, Pasqualetti F, Avanzo M. Single-fraction flattening filter-free volumetric modulated arc therapy for lung cancer: dosimetric results and comparison with flattened beams technique. *Med Dosim*. 2016;41:334–338. DOI: 10.1016/j.meddos.2016.09.002.
35. Liu H, Chen W, Lai Y, Du H, Wang Z, Xu Y, Ling Z, Fan J, Xiao P, Zhang BO, et al. Selective renal denervation guided by renal nerve stimulation in canine. *Hypertension*. 2019;74:536–545. DOI: 10.1161/HYPERTENSIONAHA.119.12680.

Supplemental Material

Data S1.

Supplemental Methods

Stereotactic body radiotherapy (SBRT) procedure for renal denervation (RDN)

Sedated animals were transported to image center and placed in lateral position. The computed tomography (CT) reference points were marked on the skin with three metallic radiopaque markers at the level of kidneys by use of wall-mounted lasers. A series of free-breathing CT scans including a native CT, a contrast-enhanced CT and a respiration-correlated 4-dimensional CT (4D-CT) were acquired on a Brilliance 16-slice CT scanner (Philips Medical Systems, Cleveland, USA) with 1 mm slice thickness. The native CT was for SBRT treatment planning. For enhanced scans to facilitate definition of target renal arteries, 50 ml contrast medium was injected (20 s delay; flow rate 2.5 ml/s, Omnipaque 350 mg I/ml, GE Healthcare, USA) through cannulated ear vein. 4D-CT obtained to assess respiration-related target motion was binned into ten respiratory phases (0-90%) with the maximum inspiration and expiration respectively corresponding to the 0% and 50% phases.

All CT images were imported to a contouring MIM workstation (MIM Software Corp., Beijing, China). The target structures defined as circumferential areas around the left and right renal arteries including aorticorenal ganglia and renal nerve were contoured in the axial planes for each slice of contrast-enhanced CT scan. These areas were combined to form a 3-dimensional clinical target volume (CTV). In addition,

organs at risk (OARs) such as kidneys, renal veins, aorta, spinal cord and bowels were delineated for protection from radiation. Contours on contrast-enhanced CT images were then transferred to 0% image sets of 4D-CT. Deformable image registration was automatically performed to propagate contours to each breathing phase with appropriate adjustment by a radiation oncologist and a cardiologist if necessary, following which the internal target volume (ITV) was generated to account for respiratory motion from maximum intensity projection image. An isotropic 3 mm expansion on ITV was used to derive the planning target volume (PTV) for setup and radiation delivery uncertainties.

The SBRT treatment plan was generated in the External Beam Planning station (Varian Medical Systems, California, USA) to deliver a total dose of 25 Gy in 2 consecutive fractions to cover most region of PTV. Doses to OARs were minimized without compromising PTV coverage or conformality. Based on the plan, radiation energy was designed to concentrate on renal arteries with rapid dose falloff away from the target.

SBRT was performed with an image-guided, volumetric modulated arc radiotherapy system (Varian Edge, Varian Medical Systems, California, USA) delivering 10-MV flattening filter-free photon beams at a dose rate of 2400 MU/min. On the treatment day, animals were initially aligned to the room lasers using skin tattoos. Before radiation delivery, a kilo-voltage cone beam CT was acquired and registered to planning CT. The registration process was performed automatically based on bony structures, followed by manual refining to ensure accurate beam

delivery as intended by the plan. The swine position was then corrected automatically according to the results of image registration, and the treatment was initiated.

Standard semi-quantitative scoring system for histopathology

All digitized histological slides were reviewed by two independent, experienced pathologists blinded to study procedure using CaseViewer version 2.0 (3DHISTECH Ltd, Budapest, Hungary). Treatment effects on renal nerves, vessels, arterioles and surrounding soft tissues were semiquantified using a standard scoring system of 0-4 proposed by Sakakura et al: 0 = none, 1 = minimal, 2 = mild, 3 = moderate, and 4 = severe^{13, 19}. The type and extent of damage to periarterial organs were routinely evaluated.

Magnitude of nerve injury was determined based on the extent of both perineural changes including inflammation or fibrosis and endoneural changes including vacuolization, pyknotic nuclei, digestion chambers, and necrosis. To investigate the lesion depth and circumferential injury achieved with radioablation, the following parameters were analyzed: (1) maximum score of nerve change in separate regions of < 2, 2-4 and > 4 mm from arterial lumen; (2) maximum distance between arterial lumen and ablation zone; (3) number of quadrants with injured nerve fascicles (score ≥ 2)/number of quadrants with nerve fascicles; (4) number of quadrants with injured periarterial soft tissue.

Arterial and venous endothelium damage was evaluated circumferentially as 0 = no endothelial loss; 1 = endothelial loss < 25% of the vessel's circumference; 2 = endothelial loss 25-50% of the vessel's circumference; 3 = endothelial loss 51-75% of

the vessel's circumference; 4 = endothelial loss > 75% of the vessel's circumference.

Medial injury was assessed separately by the depth and circumference of the involved

segments: 0 = no medial change; 1 = medial change < 25% of the medial

depth/circumference; 2 = medial change 25-50% of the medial depth/circumference; 3

= medial change 51-75% of the medial depth/circumference; 4 = medial change > 75%

of the medial depth/circumference. When evaluating the depth of arterial medial

damage, medial thinning defined as thickness of media at the site of

damage/unaffected media thickness < 0.5 was reported as absent (0) or present (1).

Meanwhile, the neointimal area of renal artery was quantitatively analyzed.

Arteriolar damage usually correlates with overall nerve damage. The scoring criteria were as follows: 0 = no injury; 1 = minimal perivascular inflammation and smooth muscle cell loss; 2 = mild perivascular inflammation and smooth muscle cell loss; 3 = moderate perivascular inflammation and segmental fibrinoid necrosis; 4 = severe perivascular inflammation and fibrinoid necrosis.

The extent of soft tissue injury characterized by the presence of denatured collagen, fat necrosis and granulation tissue was semiquantified as 0-4 according to the degree of fat necrosis, inflammation and fibrosis.

The maximum injury scores of all observational items were recorded in each section. After grading all histological sections, the maximum injury score in each vessel was determined. Mean value of scores from bilateral vessels per animal was used for statistical analysis.

Table S1. Treatment characteristics.

Case No.	Follow-up, month(s)	Treatment Time, min	PTV (Left/Right Renal Artery)					Maximum/Mean Doses to Major OARs, Gy				
			Volume, ml	Maximum Dose, Gy	Minimum Dose, Gy	CI*	HI	Left Kidney	Right Kidney	Bowel	Spinal Cord	Aorta
1	1	3.2	2.5/2.4	26.2/26.3	23.6/23.1	1.26	0.06/0.07	26.0/3.3	25.9/3.2	26.5/2.0	14.6/2.1	26.4/5.2
2	1	2.5	2.6/3.1	25.8/26.0	20.8/21.3	0.79	0.12/0.09	25.0/3.1	25.1/3.0	25.6/1.8	17.1/3.2	25.8/5.2
3	1	3.0	2.6/3.3	25.9/26.0	22.7/22.7	0.77	0.07/0.06	24.1/3.0	26.0/3.4	25.8/2.3	15.5/3.1	25.8/5.4
4	1	3.8	2.8/3.4	26.9/27.1	23.8/22.9	0.77	0.06/0.09	26.9/4.3	27.1/4.2	26.5/3.7	14.4/3.3	26.1/6.3
5	6	2.5	2.5/3.1	26.4/26.5	23.9/23.4	1.12	0.06/0.06	26.4/3.1	26.2/3.0	26.4/1.9	13.8/2.4	26.3/4.8
6	6	3.7	2.8/2.4	26.2/25.9	23.2/19.9	0.75	0.06/0.06	25.9/4.4	25.5/3.6	25.6/1.3	8.9/1.5	25.7/8.5
7	6	2.6	3.3/3.8	26.0/25.8	23.0/22.6	0.93	0.05/0.07	25.5/4.0	25.7/3.8	25.8/1.2	7.9/1.8	25.5/7.3
8	6	5.5	3.5/3.6	27.7/27.1	24.4/23.5	1.48	0.07/0.07	27.0/5.1	27.1/5.1	26.6/1.8	17.9/5.5	26.9/8.7
9	6	3.8	3.3/4.4	26.5/26.6	20.4/16.5	0.94	0.08/0.09	26.0/3.0	25.9/1.7	22.5/0.8	11.0/1.5	26.1/5.1

*CI is presented with a single value due to the same CI of radiation to bilateral renal arteries. CI, conformality index; HI, homogeneity index;

OARs, organs at risk; PTV, planning target volume.

Table S2. Radiation-induced lesion in circumference and depth.

	1 month (n = 4)	6 months (n = 5)	P value
Number of injured tissue quadrants (0-4)	3.8 ± 0.4	3.9 ± 0.2	0.633*
Injured nerve (score ≥ 2) quadrants per nerve quadrants (0-1)	0.9 ± 0.1	1.0 ± 0.1	0.515*
Maximum distance (mm)	11.6 ± 3.5	13.3 ± 0.9	0.221†

Values are expressed as mean ± SD. *P value was calculated from Mann-Whitney U

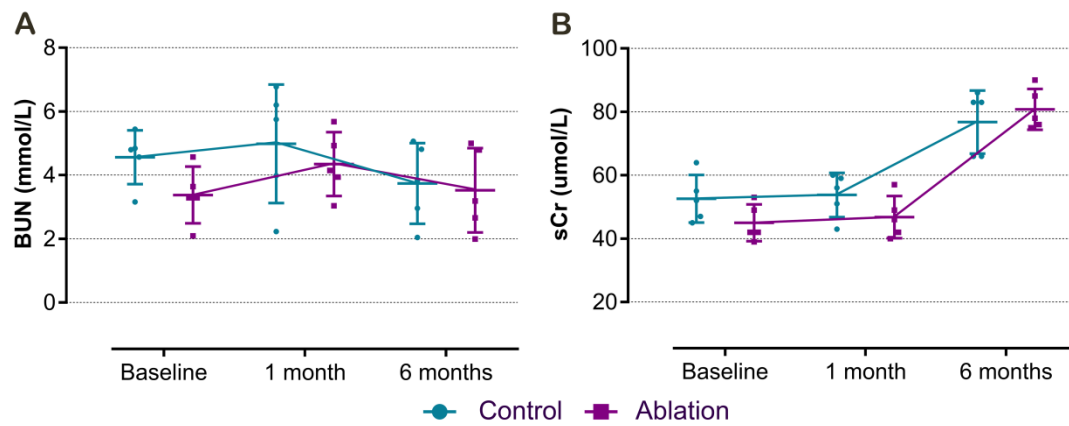
test. †P value was calculated from unpaired Student t test.

Table S3. Renal artery diameters and kidney dimensions measured from CT images at 6 months.

	Control (n = 5)	Treatment (n = 5)	P value
Renal artery diameters			
Proximal, mm	5.17 ± 0.67	4.67 ± 0.68	0.274
Middle, mm	4.66 ± 0.67	4.39 ± 0.52	0.495
Distal, mm	4.10 ± 0.37	4.23 ± 0.77	0.741
Kidney dimensions			
Craniocaudal, mm	106.66 ± 4.87	107.06 ± 6.08	0.911
Transverse, mm	45.52 ± 1.93	44.37 ± 2.70	0.460
Anteroposterior, mm	36.33 ± 3.72	33.67 ± 2.64	0.229

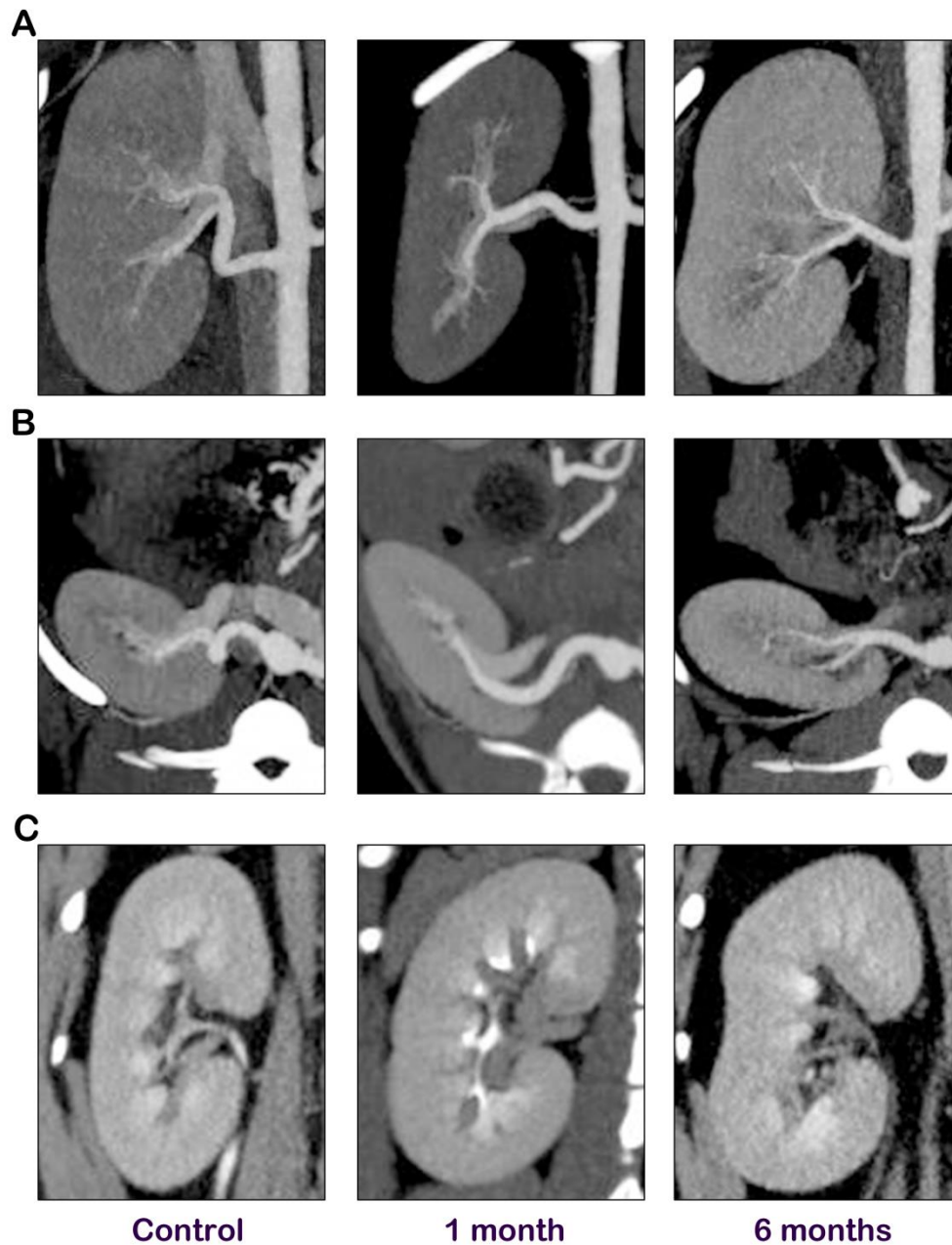
Values are expressed as mean ± SD. P value was calculated from unpaired Student t test. CT, computed tomography.

Figure S1. Renal function.



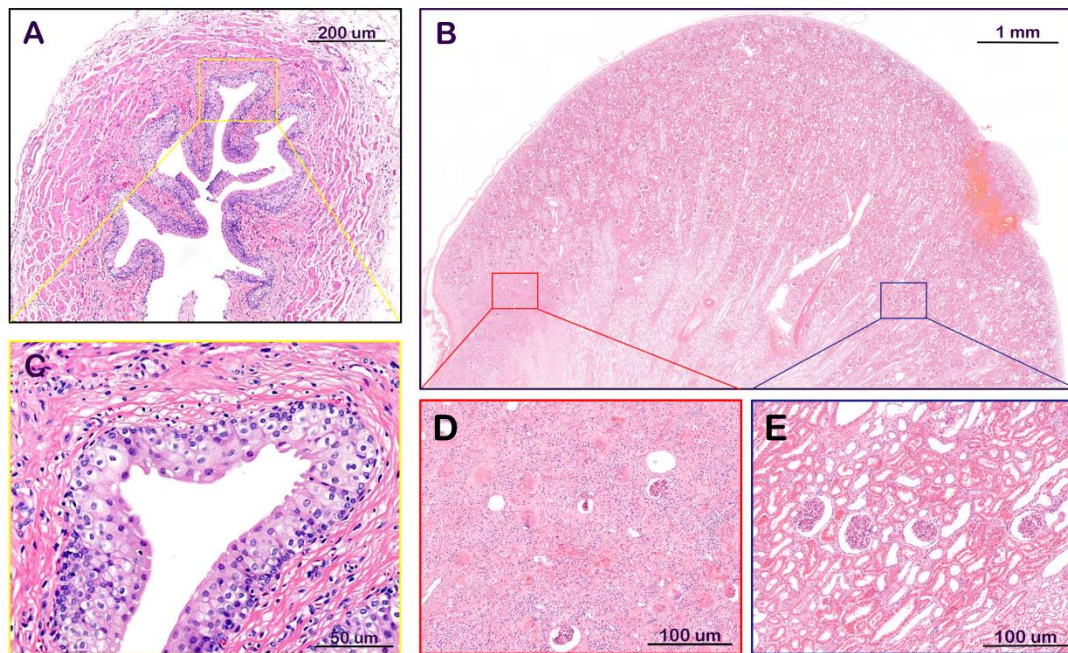
(A) Blood urea nitrogen (BUN) and (B) serum creatinine (sCr) at baseline, 1 month and 6 months follow-up in control and 6-month ablation groups (mean \pm SD; n = 5; unpaired Student t test).

Figure S2. Terminal computed tomography (CT) examination.



Representative oblique coronal (A), axial (B) and sagittal (C) multiplanar reformatting CT images in control and treatment groups showing no obvious collateral damage within 6 months after radioablation with 25 Gy.

Figure S3. Radiation-induced collateral damage.



Representative images of damage to ureter (**A**) in 1-month group and kidney (**B**) in 6-month group stained with hematoxylin and eosin. Magnified micrographs of (**C**) focal vacuolization of ureteral epithelium (yellow square in A), (**D**) kidney injury including focal glomerular vitreous degeneration, disappearance of renal tubules with inflammatory cell infiltration, interstitial fibrous tissue hyperplasia and collagen degeneration (red square in B), and (**E**) uninjured part of the kidney (blue square in B).